

Diffusion coefficient of an inclusion in a liquid membrane supported by a solvent of arbitrary thickness

Kazuhiko Seki,¹ Sanoop Ramachandran,² and Shigeyuki Komura²

¹*National Institute of Advanced Industrial Science and Technology (AIST)
AIST Tsukuba Central 5, Higashi 1-1-1, Tsukuba, Ibaraki, Japan, 305-8565*

²*Department of Chemistry, Graduate School of Science and Engineering,
Tokyo Metropolitan University, Tokyo 192-0397, Japan*

(Dated: 05/13 Received: date / Revised version: date)

Abstract

The diffusion coefficient of an inclusion in a liquid membrane is investigated by taking into account the interaction between membranes and bulk solvents of arbitrary thickness. As illustrative examples, the diffusion coefficients of two types of inclusions - a circular domain composed of fluid with the same viscosity as the host membrane and that of a polymer chain embedded in the membrane are studied. The diffusion coefficients are expressed in terms of the hydrodynamic screening lengths which vary according to the solvent thickness. When the membrane fluid is dragged by the solvent of finite thickness, via stick boundary conditions, multiple hydrodynamic screening lengths together with the weight factors to the diffusion coefficients are obtained from the characteristic equation. The condition for which the diffusion coefficients can be approximated by the expression including only a single hydrodynamic screening length are also shown.

I. INTRODUCTION

Recent advances in experimental techniques have made the direct observation of the Brownian motion of μm sized objects in membranes using microscopy and imaging a routine process [1–7]. As a result, diffusion coefficients can be measured accurately and it is now possible to address the issue of the differences between Brownian motion of macromolecules embedded in membranes in various environments.

Vesicles with sizes of the order of $10\ \mu\text{m}$ are frequently used in experiments while the typical distance of a supported membrane from the substrate is of the order of $20\ \text{\AA}$ [5, 6]. Obviously, in both these general cases the coupling of membrane with its environment are very different and hence it will influence the Brownian motion of inclusions. In this paper, we investigate the influence of solvent environments on diffusion of an inclusion embedded in a membrane. In the biological context, there are many examples of membranes coming in contact with a solvent of various depth such as in tissues.

Biological membranes can be regarded as two-dimensional (2D) viscous fluids. An important feature of membranes as a transport media is that they are not purely isolated [12–14]. Liquid membranes are coupled to surrounding solvents by interaction of polar head groups of lipid molecules with solvents; they form quasi-2D systems coupled to three-dimensional (3D) solvents. The coupling to the surrounding environments induces the momentum exchange between the membrane and the solvents. The influence of the momentum exchange on the Brownian dynamics has been theoretically investigated by introducing a phenomenological coupling constant or simplifying the solvents flow [8–17]. These studies have also been extended to investigate the concentration fluctuations [18, 19, 22].

Despite the large number of studies, the Brownian motion of an object in liquid membranes has not yet been fully understood. In a hydrodynamic description, 2D flow in a bilayer membrane can be regarded as viscous and the interaction between liquid membranes and surrounding solvents can be taken into account by the stick boundary condition between them. Diffusion coefficients of macroscopic inclusions embedded in membranes were analytically investigated for a planar membrane surrounded by solvent layers of infinite [8–11] or very small thickness [12–17]. These studies revealed that the hydrodynamic flow in a membrane is screened by the solvent drag force and is characterized by a hydrodynamic screening length. When a planar membrane is surrounded by infinite thickness of solvent,

it is called the Saffman and Delbrück (SD) hydrodynamic screening length, ν^{-1} , and is given by the ratio between the 2D membrane viscosity η and the 3D solvent viscosity η_s , $\nu^{-1} = \eta/\eta_s$ [8, 9]. (As we shall see below, the dimension of the 2D membrane viscosity is that of 3D solvent viscosity times a length.) In the opposite limit of a thin solvent layer of the thickness h , Evans and Sackmann (ES) hydrodynamic screening length given by $\sqrt{h/\nu}$ is appropriate [14]. In both limits, the diffusion coefficients depend logarithmically on the size of the inclusions as long as the size is smaller than the hydrodynamic screening length. On the other hand, the diffusion coefficients depend on the size of the inclusions very differently when the size of the inclusions exceeds the hydrodynamic screening length. These studies naturally lead to the interest in the hydrodynamic screening length and its influence on the diffusion coefficients when the solvent layer has a finite thickness.

The solvent flow can be varied by changing the solvent thickness. The flow of solvents influences the membrane flow through the stick boundary condition imposed between the membrane and the solvents. As a result, the diffusion coefficients depend on the solvent thickness. The influence of the finite solvent thickness has been recently studied for diffusion of a disk [20], concentration fluctuations [21–23], correlated diffusion [24–27], and polymer diffusion in a membrane [28]. Diffusion coefficients of other types of inclusions on membranes [17, 29–32] or on Langmuir monolayers [33] have also been theoretically calculated. However, the investigation on the influence of finite thickness of solvent was limited to numerical evaluation of the diffusion coefficients, where the dependence of the hydrodynamic screening length on the solvent thickness was not completely elucidated [20–28]. In this paper, the relation between the diffusion coefficients and the hydrodynamic screening lengths are thoroughly investigated for an arbitrary thickness of the solvent layers on the basis of the analytical expression on the hydrodynamic screening lengths.

The relation between the diffusion coefficients and the hydrodynamic screening lengths can be shown in a straight-forward manner for a polymer embedded in a membrane by the Zimm model, where the equilibrium average of the hydrodynamic interactions is performed in 2D [17, 28, 31]. The multiple hydrodynamic screening lengths are then found for the finite solvent thickness. The diffusion coefficients are expressed by the weighted sum; each term in the sum is a product of the weight factor and the function of the dimensionless size of the polymer normalized by each hydrodynamic screening length. On the basis of the analytical expression, the condition that the diffusion coefficient is approximately represented solely

by the ES hydrodynamic screening length can be discussed in detail. We show that the diffusion coefficient cannot be approximated by the ES hydrodynamic screening length when both $\nu^{-1} = \eta/\eta_s$ and the size of the macromolecule are smaller than the solvent thickness.

Essentially the same relation between the diffusion coefficients and the hydrodynamic screening lengths is obtained for diffusion of a circular liquid domain with the same viscosity as that of the host membrane. The diffusion coefficient of a circular liquid domain embedded in a membrane has been studied in relation to recently proposed raft model, where rafts are formed by sphingomyelin and cholesterol rich liquid domains [1, 6, 7, 34–38]. It is believed that rafts undergo lateral Brownian motion within a bilayer membrane and act as platforms for protein association and signaling [35]. Previously, the diffusion coefficient of a circular liquid domain of arbitrary size was derived in the limit of infinite depth of solvent layer or the limit of small depth of solvent layer [7, 16, 39, 40]. In this paper, the results are generalized for the arbitrary thickness of solvent layers. The diffusion coefficient is obtained as a simple integral which can be expressed again as the sum of the terms given by functions of the same hydrodynamic screening lengths multiplied by the same weight factors as those for the polymer diffusion coefficients.

In Sec. II, the membrane hydrodynamics is reviewed. The diffusion coefficient of a polymer embedded in a membrane is obtained in Sec. III. In Sec. IV, the relation between hydrodynamic screening length and the solvent thickness is discussed. The diffusion coefficient of a liquid domain in a membrane is obtained in Sec. V. Finally, the last section is devoted to conclusions.

II. HYDRODYNAMIC FLOW IN A MEMBRANE AND SOLVENT

As shown in Fig. 1, we consider the situation where the liquid membrane is supported by a bulk solvent on the solid substrate. The situation where the membrane is also supported by a solvent from above will be considered in Sec. VI. We denote the 2D flow in the membrane by $\mathbf{v}(\mathbf{r})$ where $\mathbf{r} = (x, y)$ represents a position within the plane of the membrane. The membrane is regarded to be incompressible,

$$\nabla \cdot \mathbf{v}(\mathbf{r}) = 0. \tag{1}$$

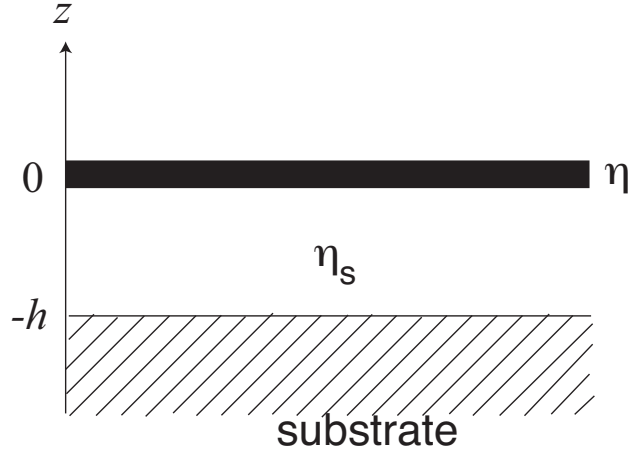


FIG. 1. Schematic picture showing a planar liquid membrane with 2D viscosity η located at $z = 0$. It is supported on a solvent with 3D viscosity η_s . A substrate is located at $z = -h$ bounding the solvent.

Here ∇ is a differential operator in the 2D Euclidean space. The viscous flow in the membrane can be expressed by the Stokes equation in 2D,

$$\eta \nabla^2 \mathbf{v}(\mathbf{r}) - \nabla p(\mathbf{r}) + \mathbf{f}_s(\mathbf{r}) = 0, \quad (2)$$

where η is the 2D membrane viscosity, $p(\mathbf{r})$ the in-plane pressure, and $\mathbf{f}_s(\mathbf{r})$ the in-plane force exerted on the membrane from the solvent. The last quantity can be obtained when the solvent fluid velocities are determined. The stress tensor of the liquid membrane is given by

$$\sigma_{\alpha\beta}(\mathbf{r}) = -p(\mathbf{r})\delta_{\alpha\beta} + \eta[\partial_\alpha v_\beta(\mathbf{r}) + \partial_\beta v_\alpha(\mathbf{r})], \quad (3)$$

where $\delta_{\alpha\beta}$ is the Kronecker delta, and α, β are x, y . Then Eq. (2) can be represented in terms of the stress tensor as,

$$\text{div } \boldsymbol{\sigma} + \mathbf{f}_s(\mathbf{r}) = 0, \quad (4)$$

where $(\text{div } \boldsymbol{\sigma})_\alpha = \sum_\beta \partial \sigma_{\alpha\beta} / \partial x_\beta$.

As shown in Fig. 1, the membrane is located in the plane at $z = 0$. The solvent velocities $\mathbf{v}^{(3)}(\mathbf{r}, z)$, satisfy the incompressibility condition

$$\tilde{\nabla} \cdot \mathbf{v}^{(3)}(\mathbf{r}, z) = 0, \quad (5)$$

where $\tilde{\nabla}$ represents a differential operator in the 3D Euclidean space. We denote the 3D viscosity of the solvent as η_s , and the solvent flow also obeys the 3D Stokes equation,

$$\eta_s \tilde{\nabla}^2 \mathbf{v}^{(3)}(\mathbf{r}, z) - \tilde{\nabla} p^{(3)}(\mathbf{r}, z) = 0, \quad (6)$$

where $p^{(3)}(\mathbf{r}, z)$ represents the pressure of the solvent. The solvent is supported on the substrate which is located at $z = -h$. The no-slip boundary condition is imposed at $z = -h$ as well as between the membrane flow and the solvent flow. Through this boundary condition, the surrounding solvent exerts a drag force on the liquid membrane.

The drag force in Eq. (2) can be expressed as $\mathbf{f}_s = -(\mathbf{I} - \hat{\mathbf{e}}_z \hat{\mathbf{e}}_z) \cdot \sigma^{(3)}(\mathbf{r}, 0) \cdot \hat{\mathbf{e}}_z$, where $\hat{\mathbf{e}}_z$ is the unit vector along the z -axis. The tensorial component of \mathbf{I} is given by δ_{ij} , and $\mathbf{I} - \hat{\mathbf{e}}_z \hat{\mathbf{e}}_z$ denotes the projection to the in-plane space. The stress tensor of solvent is given by

$$\sigma_{ij}^{(3)}(\mathbf{r}, z) = -p^{(3)}(\mathbf{r}, z) \delta_{ij} + \eta_s [\tilde{\partial}_i v_j^{(3)}(\mathbf{r}, z) + \tilde{\partial}_j v_i^{(3)}(\mathbf{r}, z)], \quad (7)$$

where i, j denote x, y, z .

Using the stick boundary conditions at $z = 0$ and $z = -h$, we solve the hydrodynamic equations from Eq. (5) to Eq. (6) to obtain \mathbf{f}_s . In the Fourier space, \mathbf{f}_s is calculated to be [22, 33, 41]

$$\mathbf{f}_s[\mathbf{k}] = -\eta_s k \coth(kh) \mathbf{v}[\mathbf{k}], \quad (8)$$

where $\mathbf{k} = (k_x, k_y)$ and $k = |\mathbf{k}|$. The real space velocity field of the membrane flow $\mathbf{v}(\mathbf{r})$ can be expressed as

$$\mathbf{v}(\mathbf{r}) = \int \frac{d^2k}{(2\pi)^2} \mathbf{v}[\mathbf{k}] \exp(i\mathbf{k} \cdot \mathbf{r}). \quad (9)$$

The Fourier space mobility tensor $\mathbf{G}[\mathbf{k}]$ associated with the velocity field is given by [22, 33, 41]

$$G_{\alpha\beta}[\mathbf{k}] = \frac{1}{\eta[k^2 + \nu k \coth(kh)]} \left(\delta_{\alpha\beta} - \frac{k_\alpha k_\beta}{k^2} \right). \quad (10)$$

In order to calculate diffusion coefficients, the mobility tensor in Fourier space should be transformed into real space. Previously, the inverse Fourier transform of the mobility tensor was analytically performed only in the limits of infinite or zero thicknesses of a solvent layer. In the next section, the inverse Fourier transformation of the mobility tensor is analytically performed for an arbitrary thickness of a solvent.

III. DIFFUSION COEFFICIENT OF A 2-DIMENSIONAL POLYMER CHAIN

As an illustrative example for the influence of finite thickness of solvent on the diffusion coefficient of a macromolecule embedded in a 2D planar membrane, we consider the diffusion of a polymer chain confined in the membrane [17, 28, 31]. Previously, the influence of the solvent on diffusion coefficients is analytically investigated only in the limits of very thin or infinite thicknesses of solvent layers. In these works, the hydrodynamic screening length is a key quantity in characterizing the screening of the flow of membrane by the presence of solvent layers. The influence of finite thickness of solvent was investigated by numerically evaluating the inverse Fourier transform of the mobility tensor, where the hydrodynamic screening length was not even defined. In this section, the hydrodynamic screening lengths are obtained from an analytical equation for arbitrary thickness of solvent layer.

The conformation of a 2D polymer chain embedded in a 2D membrane is represented by N beads with position vectors, $\{\mathbf{R}_n\} = (\mathbf{R}_1, \dots, \mathbf{R}_N)$, under the potential energy,

$$U = \frac{k_B T}{b^2} \sum_{n=2}^N (\mathbf{R}_n - \mathbf{R}_{n-1})^2, \quad (11)$$

where b is the Kuhn length [42]. The mobility tensor associated with the beads is given by the inverse Fourier transform of Eq. (10) as

$$G_{\alpha\beta}(\mathbf{R}_n - \mathbf{R}_m) = \int \frac{d^2k}{(2\pi)^2} G_{\alpha\beta}[\mathbf{k}] \exp[i\mathbf{k} \cdot (\mathbf{R}_n - \mathbf{R}_m)]. \quad (12)$$

Within the pre-averaging approximation [42], the polymer diffusion coefficient is expressed as

$$D_{\text{poly}} = k_B T \int_0^N \frac{dn}{N} \int_0^N \frac{dm}{N} g(n - m), \quad (13)$$

where $g(n - m)$ is the isotropic component of mobility tensor $G_{\alpha\beta}(\mathbf{R}_n - \mathbf{R}_m)$ [28]. By using Eq. (12), two analytical expressions for the diffusion coefficients have been derived from Eq. (13) in the limits of very thin or infinite thickness of solvent layers [17, 28]. Here, we investigate the diffusion coefficient by keeping the finite depth of the solvent layer without taking the limits. By expanding $1/[k + \nu \coth(kh)]$ in partial fractions, we note the general relation [43]

$$\int_0^\infty dk \frac{f(k)}{k + \nu \coth(kh)} = \sum_{j=1}^\infty C_j \int_0^\infty dk \frac{k f(k)}{k^2 + \kappa_j^2}, \quad (14)$$

where $f(k)$ is an arbitrary function, κ_j and C_j will be later given by Eqs. (16) and (17), respectively. By introducing Eq. (14) into Eqs. (12) and (13), we obtain,

$$g(n-m) = - \sum_{j=1}^{\infty} C_j \frac{1}{8\pi\eta} \exp\left(\frac{1}{4}b^2\kappa_j^2|n-m|\right) \times \text{Ei}\left(-\frac{1}{4}b^2\kappa_j^2|n-m|\right), \quad (15)$$

where $\text{Ei}(-z)$ is the exponential integral [44].

In the real space, the mobility tensor is expressed in terms of an infinite number of characteristic lengths, κ_j^{-1} , where κ_j is determined by the following characteristic equation

$$\cot(\kappa_j h) = \frac{\kappa_j}{\nu}. \quad (16)$$

All the roots of the equation are given by $\kappa = \pm\kappa_j$ with $j = 1, 2, \dots$. The characteristic lengths relative to h , $1/(\kappa_j h)$, depend on νh given by the viscosity ratio $\nu = \eta_s/\eta$, and represent the screening of hydrodynamic flow in 2D membrane due to the presence of the solvent. The contribution of each screening length is weighted by the factor

$$C_j = \frac{2\nu}{h\kappa_j^2 + h\nu^2 + \nu}. \quad (17)$$

Using Eq. (15), the diffusion coefficient is obtained as

$$D_{\text{poly}} = \sum_{j=1}^{\infty} C_j \frac{k_B T}{4\pi\eta} \frac{1}{\epsilon_j^4} \left[(1 + \epsilon_j^2)(2 \ln \epsilon_j + \gamma) - \epsilon_j^2 - \exp(\epsilon_j^2) \text{Ei}(-\epsilon_j^2) \right], \quad (18)$$

where $\gamma = 0.5772 \dots$ is Euler's constant. In the above, we have defined the dimensionless polymer size as $\epsilon_j \equiv \sqrt{N}b\kappa_j/2 = R_g\kappa_j$, and $R_g = \sqrt{N}b/2$ is the radius of gyration for the 2D Gaussian polymer chain.

The limiting expression for $\epsilon_1 \ll 1$ is

$$D_{\text{poly}} \approx C_1 \frac{k_B T}{4\pi\eta} \left[-\ln \epsilon_1 - \frac{\gamma}{2} + \frac{3}{4} \right]. \quad (19)$$

As will be discussed in the next section, the above expression is close to the exact result under the additional condition of $\nu h < 1$ which is needed to replace the sum in Eq. (18) with the term related to ϵ_1 . When $\epsilon_1 \gg 1$, Eq. (18) reduces to

$$D_{\text{poly}} \approx C_1 \frac{k_B T}{4\pi\eta} \frac{1}{\epsilon_1^2} \left[2 \ln \epsilon_1 + \gamma - 1 \right]. \quad (20)$$

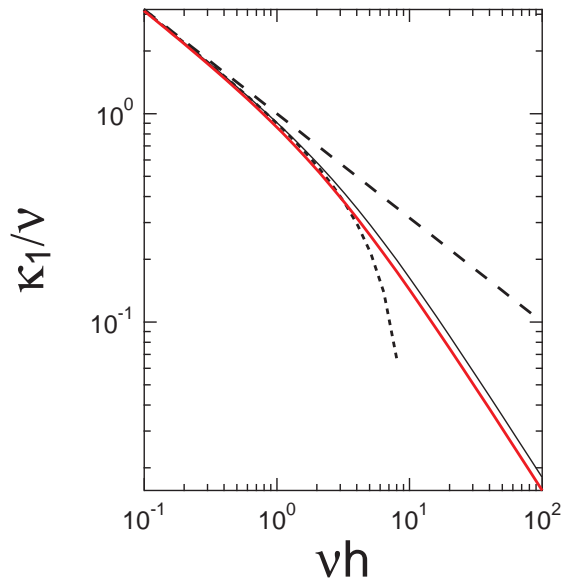


FIG. 2. (Color online) The smallest positive values for the inverse of the characteristic lengths against the solvent thickness. Both quantities are normalized by $\nu = \eta_s/\eta$. The red thick line represents the smallest positive root of the characteristic equation, Eq. (16), calculated numerically. The long dashed line represents $\kappa/\nu = 1/\sqrt{\nu h}$. The short dashed line represents the result of Eq. (23). The thin solid line represents the result of Eq. (22).

This expression holds regardless of the value of h as long as it is finite. The sum in Eq. (18) can be represented by the single dominant term as long as $\epsilon_1 \gg 1$. However, the additional condition of $\nu h < 1$ is required when $\epsilon_1 \ll 1$, about which we shall discuss in the next section.

IV. HYDRODYNAMIC SCREENING LENGTH VS. SOLVENT THICKNESS

If the approximated diffusion coefficient obtained by taking into account only the smallest positive value of κ_j (denoted by κ_1) reproduce the exact results, then κ_1^{-1} can be regarded as the effective hydrodynamic screening length.

First, we consider the value of κ_1 which is the inverse of the effective hydrodynamic screening length as long as the higher order ($j \geq 2$) terms can be ignored. We first note the

series expansion,

$$x \cot x = 1 + 2 \sum_{n=1}^{\infty} \frac{x^2}{x^2 - n^2 \pi^2}. \quad (21)$$

Since the lowest order term can be estimated as $1 + 2x^2/(x^2 - \pi^2) \approx x^2/(\nu h)$, the approximate expression for κ_1 turns out to be

$$\kappa_1 \approx \left(\frac{3\nu h + \pi^2 - \sqrt{(3\nu h)^2 + 2\nu h \pi^2 + \pi^4}}{2h^2} \right)^{1/2}. \quad (22)$$

In the limit of $\nu h/\pi^2 < 1$, κ_1 can be further approximated as

$$\kappa_1 \approx \kappa \left(1 - \frac{\nu h}{\pi^2} \right), \quad (23)$$

where $\kappa = \sqrt{\nu/h}$ is the inverse of the ES hydrodynamic screening length defined in the limit of $h \rightarrow 0$. In Fig. 2, the smallest positive values for the inverse of the characteristic lengths are presented against the solvent layer thickness, h . By increasing the solvent layer thickness h , the inverse of the hydrodynamic screening length rapidly decreases as shown in Fig. 2.

Next we consider the condition for which the diffusion coefficient can be characterized by a single hydrodynamic screening length as a good approximation for the exact expression including multiple hydrodynamic screening lengths associated with higher order κ_j . Judging from Eq. (16) and Fig. 3 (a), κ_j takes discrete values which are almost equally separated. When $\kappa_1 R_g$ is well separated from $\kappa_2 R_g$ and the diffusion coefficient is given by the weighted sum of monotonically decreasing functions of $\kappa_j R_g$ multiplied by the rapidly decreasing weights, the sum can be well represented by the term associated with $\kappa_1 R_g$ alone. Below, we show that $\kappa_1 R_g$ is well separated from $\kappa_2 R_g$ when $R_g > h$ and the weights rapidly decay when $h < 1/\nu$.

Since we have $\kappa_j \approx \kappa_1 + \pi(j-1)/h$, the hydrodynamic screening lengths are separated by the factor $1/h$. Hence $\kappa_2 R_g$ is well separated from $\kappa_1 R_g$ when $R_g/h > 1$. It is convenient to define the cut-off size $R_g^* = h$ over which the expression with $\kappa_1 R_g$ could be very different from that with $\kappa_2 R_g$.

In Fig. 3 (b), the weight factors C_j are shown against κ_j/ν . The weight factors C_j in Eq. (17) decrease with increasing κ_j . The ratio of C_2/C_1 is an important factor in estimating whether the term related to κ_1 is dominant over other terms. Fig. 3 (b) shows that the difference between C_1 and C_2 increases by decreasing the thickness of solvent layer.

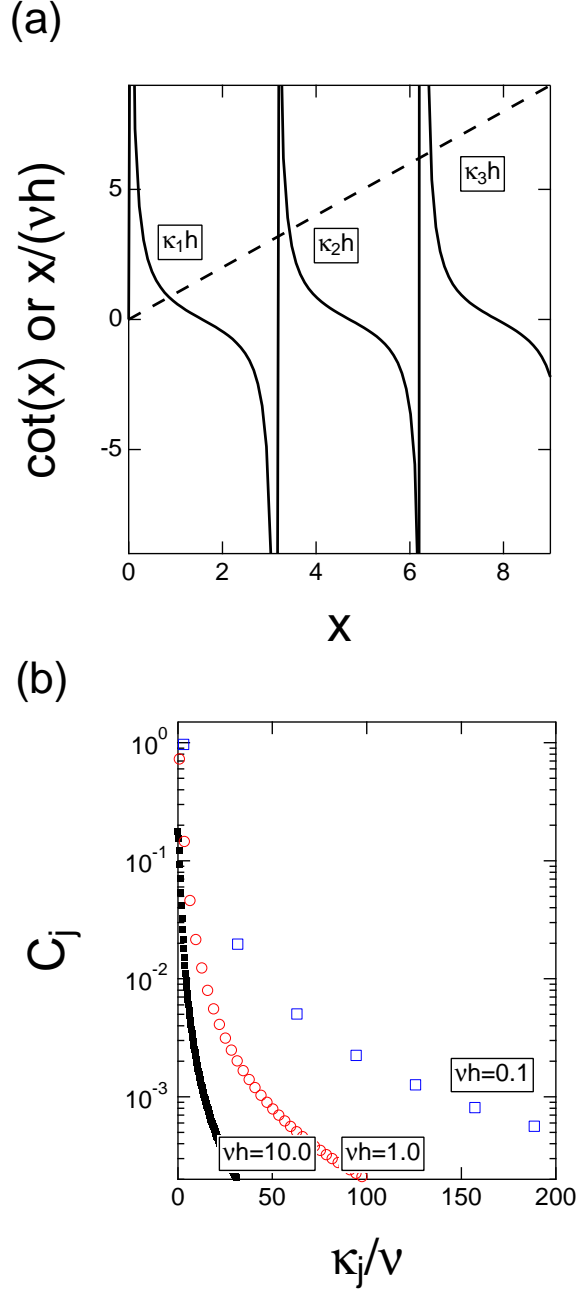


FIG. 3. (Color online)

(a) The pictorial solution of the characteristic equation, Eq. (16); $\cot(x)$ against x and $x/(\nu h)$ against x for $\nu h = 1$. The cross points of lines are $x_j = \kappa_j h$. The smallest positive value is x_1 . κ_1 is obtained by $\kappa_1 = x_1/h$ (b) C_j against κ_j/ν . C_j represents the weight associated with each hydrodynamic screening length, Eq.(17). Blue squares, red circles and dots represent $\nu h = 0.1$, $\nu h = 1.0$ and $\nu h = 10.0$, respectively.

Specifically, we have $\kappa_j \approx \kappa_1 + \pi(j-1)/h$ and $C_2/C_1 \approx \kappa_1^2/\kappa_2^2 \approx \nu h/\pi^2$. Hence the diffusion coefficient can be approximated by the expression involving κ_1 alone when $\nu h/\pi^2 < 1$. When the condition $\nu h < 1$ is satisfied, $C_2/C_1 < 1$ and the diffusion coefficients can be approximated by those obtained by Evans and Sackmann, where $C_1 \sim 1/(1 + \nu h/2) \sim 1$. It is then convenient to define the critical thickness of solvent $h^* = 1/\nu$. If the solvent depth exceeds h^* , the weight of C_2 is not much different from that of C_1 . It should be noticed, however, that the precise estimation of the contribution from the higher modes requires the whole expression besides the weights.

The expression of the diffusion coefficient depends on the kind of inclusions. As a representative example, we consider the diffusion coefficient of polymer to study conditions to use a single effective hydrodynamic screening length given by $1/\kappa_1$. In Fig. 4, we show the polymer diffusion coefficients against the size of the polymer R_g to study whether the polymer diffusion coefficients can be approximated by an expression without summation. When $\nu h \leq 1$, the polymer diffusion coefficients can be approximated by taking into account only κ_1 as shown in Fig. 4. It is consistent with the fact that the weight C_2 is smaller than C_1 when $\nu h \leq 1$ since $C_2/C_1 \sim \nu h/\pi^2$. The situation corresponds to that considered by Evans and Sackmann.

When $\nu h > 1$, C_1 is close to C_2 and the functional form of the diffusion coefficient should be carefully examined. When $\nu h > 1$ and $R_g > h$ holds, $\kappa_1 R_g > 1$ is satisfied. Then the diffusion coefficient is well approximated by Eq. (20) showing $1/(\kappa_1 R_g)^2$ dependence. Notice that $1/(\kappa_j R_g)^2$ decays relatively fast by increasing j . When $\nu h > 1$ and the size of the polymer R_g exceeds the solvent thickness h , the diffusion coefficient is approximated by the expression given in terms of $\kappa_1 R_g$ alone.

When $\nu h > 1$ and $R_g < h$, on the other hand, a significant deviation is seen for the diffusion coefficients if the higher order terms are ignored, as can be seen from Fig. 4. This deviation originates from the fact that the weak logarithmic dependence on $\kappa_j R_g$ and $\kappa_2 R_g$ is not well separated from $\kappa_1 R_g$ if $R_g/h < 1$. Also notice that C_1 is close to the other values of C_j if $\nu h > 1$. In such a situation, multiple hydrodynamic screening lengths should be taken into account.

To summarize, we have four length scales: the critical thickness of the solvent $h^* = \nu^{-1}$, the cut-off size of the polymer $R_g^* = h$, the SD hydrodynamic screening length ν^{-1} , and the ES hydrodynamic screening length κ_1^{-1} (see Eq. (22)). Although h^* is identical to the

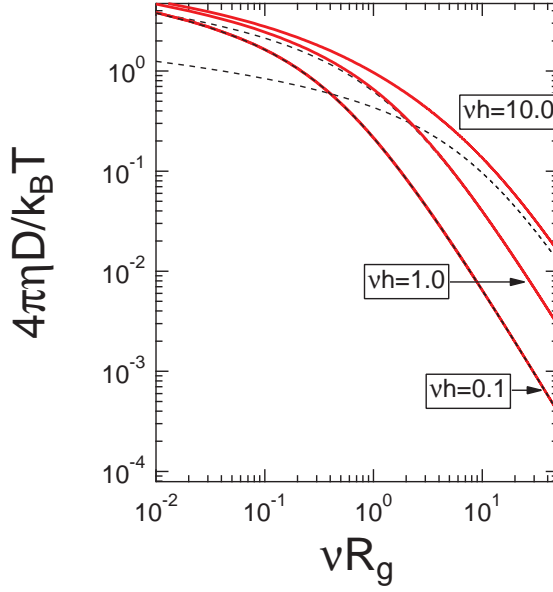


FIG. 4. (Color online) The diffusion coefficients of polymer against size for various solvent thickness. The solid red lines indicate the complete solution obtained from Eq. (18). The short dashed black lines indicate the approximate solution by assuming a characteristic length scale for hydrodynamic screening given by $1/\kappa_1$. The short dashed line for $\nu h = 0.1$ overlaps with the exact solution.

SD hydrodynamic screening length ν^{-1} , their physical meanings are different as explained below.

The diffusion coefficient can be approximately expressed by using either ν^{-1} or κ_1^{-1} . For the thin solvent layer, $h < 1/\nu$, the weights rapidly decrease with increasing j and the diffusion coefficient is given by κ_1^{-1} regardless of the macromolecule size. This is the limiting case considered by Evans and Sackmann. For thick solvent layers exceeding the critical thickness $h^* = 1/\nu$, the diffusion coefficient can be approximated by the expression including only the single hydrodynamic screening length κ_1^{-1} , when the size of the macromolecule is larger than $R_g^* = h$. In this case, we have $(\kappa_2 - \kappa_1)R_g \sim R_g/h > 1$ and $\kappa_1 R_g$ is well separated from $\kappa_2 R_g$. When the solvent thickness exceeds $h^* = 1/\nu$ and the size of macromolecules is smaller than $R_g^* = h$, on the other hand, the diffusion coefficient shows weak logarithmic dependence on $\kappa_j R_g$ and multiple hydrodynamic screening lengths should be taken into account. The diffusion coefficient is expressed by the hydrodynamic screening length ν^{-1} in the limit of $h \rightarrow \infty$.

V. DIFFUSION COEFFICIENT OF A CIRCULAR DOMAIN

In this section, we consider the diffusion coefficient of a circular liquid domain in a membrane (see Fig. 5). Although the characteristic equation, Eq. (16) associated with the solvent and the membrane flow should not be altered by changing the inclusion from polymers to liquid domains, the condition that the diffusion coefficient can be approximated by truncating the infinite sum to a single expression depends on the size dependence of the diffusion coefficients. The size dependence can differ between polymers and liquid domains. For simplicity, we consider the case when the viscosity of the circular liquid domain is the same as that of the host membrane denoted by η . Previously, simple expressions for the diffusion coefficients were obtained for either infinite or very thin limits of the solvent layers [16, 39]. Here we generalize the results to arbitrary thickness of solvent layers.

We consider the situation for which the center of the circular object moves with the velocity \mathbf{U} , and its edge is assumed to keep circular shape without any deformation. The velocity field inside and outside the circular domain satisfy [45]

$$\eta \nabla^2 \mathbf{v}(\mathbf{r}) - \nabla p(\mathbf{r}) + \mathbf{f}_s(\mathbf{r}) + \mathbf{F}^{(\ell)}(\mathbf{r}) \frac{\delta(r-R)}{2\pi R} = 0, \quad (24)$$

and the incompressibility condition given by Eq. (1) for all \mathbf{r} . Here \mathbf{f}_s was defined before in Eq. (8), and $\mathbf{F}^{(\ell)}$ is the force exerted at the periphery of the circle in the direction normal to the circular boundary [39]. If we take the origin of the coordinates at the center of the circular domain and choose the x -coordinate in the direction of \mathbf{U} , $\mathbf{F}^{(\ell)}$ should vary according to the velocity \mathbf{U} at the periphery of the circle. From the symmetry with respect to \mathbf{U} , $\mathbf{F}^{(\ell)}$ can be expressed as [39]

$$\mathbf{F}^{(\ell)}(\mathbf{r}) = F^{(\ell n)} \cos \theta \mathbf{n}, \quad (25)$$

where $\mathbf{n} = \mathbf{r}/r$ is the outward normal unit vector at the surface of the circle of radius R , and θ is the angle between \mathbf{U} and \mathbf{r} .

Our task is to calculate the total force exerted on the circular domain in the steady state

$$\mathbf{F} = \int_{r \leq R} d\mathbf{r} \mathbf{f}_s + \int_{r=R} d\ell \boldsymbol{\sigma} \cdot \mathbf{n}, \quad (26)$$

where $\boldsymbol{\sigma}$ is the stress tensor of the liquid membrane given by Eq. (3) and $d\ell$ denotes the line integration. The first term represents the force exerted from the membrane flow field, and the second term represents the direct friction force exerted from the solvent surrounding the membrane to the circular domain.

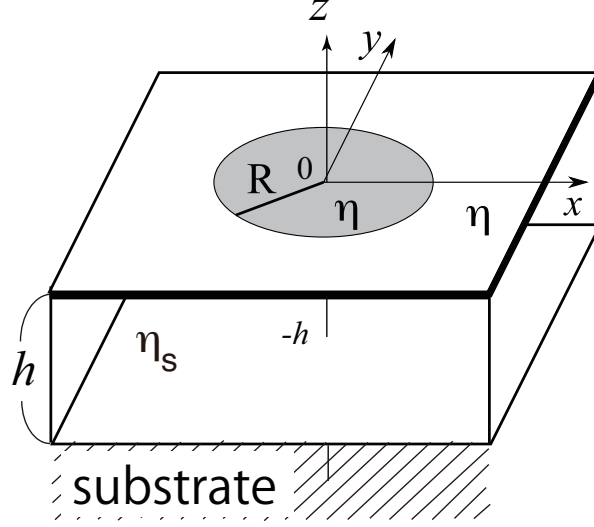


FIG. 5. Schematic picture showing a liquid domain embedded in a planar liquid membrane located at $z = 0$. Both a liquid domain and a membrane have the same 2D viscosity η . It is supported on a solvent with 3D viscosity η_s . A substrate is located at $z = -h$ bounding the solvent in the lower region.

By using Gauss's theorem, we find

$$\begin{aligned}
 \mathbf{F} &= \int_{r=R} d\ell \boldsymbol{\sigma} \cdot \mathbf{n} + \int_{r \leq R} d\mathbf{r} \mathbf{f}_s \\
 &= \int_{r \leq R} d\mathbf{r} \operatorname{div} \boldsymbol{\sigma} + \int_{r \leq R} d\mathbf{r} \mathbf{f}_s \\
 &= - \int_{r \leq R} d\mathbf{r} \mathbf{F}^{(\ell)}(\mathbf{r}) \frac{\delta(r-R)}{2\pi R} \\
 &= -F^{(\ell n)} \hat{\mathbf{e}}_x \int_0^{2\pi} \frac{d\theta}{2\pi} \cos^2 \theta = -\frac{F^{(\ell n)}}{2} \hat{\mathbf{e}}_x,
 \end{aligned} \tag{27}$$

where Eq. (4) and Eq. (24) are used to obtain the third equality, and $\hat{\mathbf{e}}_\alpha$ denotes the unit vector along the α -direction. Equation (27) shows that it is sufficient to calculate $F^{(\ell n)}$ to obtain the total force exerted on the circular object from the membrane flow field and the

solvent.

The velocity field can be formally expressed as

$$v_\alpha(\mathbf{r}) = \int d\mathbf{r}' G_{\alpha\beta}(\mathbf{r} - \mathbf{r}') F_\beta^{(\ell)}(\mathbf{r}') \frac{\delta(r' - R)}{2\pi R}. \quad (28)$$

In real space, the mobility tensor is expressed by the Fourier transform of Eq. (10) as

$$G_{\alpha\beta}(\mathbf{r}) = \int \frac{d^2k}{(2\pi)^2} G_{\alpha\beta}[\mathbf{k}] \exp(i\mathbf{k} \cdot \mathbf{r}). \quad (29)$$

Equation (28) can be rewritten as

$$v_\alpha(\mathbf{r}) = \int \frac{d^2k}{(2\pi)^2} \int d\mathbf{r}' \exp(i\mathbf{k} \cdot \mathbf{r}) G_{\alpha\beta}[\mathbf{k}] \exp(-i\mathbf{k} \cdot \mathbf{r}') \times F_\beta^{(\ell)}(\mathbf{r}') \frac{\delta(r' - R)}{2\pi R}. \quad (30)$$

Let φ denote the angle between \mathbf{r}' and \mathbf{U} . Then we obtain

$$\begin{aligned} & \int d\mathbf{r}' \exp(-i\mathbf{k} \cdot \mathbf{r}') F_\beta^{(\ell)}(\mathbf{r}') \frac{\delta(r' - R)}{2\pi R} \\ &= \int_0^{2\pi} \frac{d\varphi}{2\pi} \exp[-i(k_x \cos \varphi + k_y \sin \varphi) R] F^{(\ell n)} \cos \varphi \frac{r'_\beta}{r'}, \end{aligned} \quad (31)$$

where \mathbf{r}'/r' is the unit orientational vector. Equation (30) can be rewritten by using Eq. (31) and the relation

$$\left(\delta_{\alpha\beta} - \frac{k_\alpha k_\beta}{k^2} \right) \frac{r'_\beta}{r'} = \frac{r'_\alpha}{r'} - \frac{k_\alpha}{k^2} (k_x \cos \varphi + k_y \sin \varphi). \quad (32)$$

The integration with respect to φ can be performed (see Appendix for the useful relations to perform this integration), and the result becomes

$$\begin{aligned} \mathbf{v}(\mathbf{r}) &= \int \frac{d^2k}{(2\pi)^2} \frac{\exp(i\mathbf{k} \cdot \mathbf{r})}{\eta[k^2 + \nu k \coth(kh)]} \left[\frac{k_y^2}{k^3 R} J_1(kR) \hat{\mathbf{e}}_x \right. \\ &\quad \left. + \left(\frac{k_y}{k^2} J_2(kR) - \frac{k_x k_y}{k^3 R} J_1(kR) \right) \hat{\mathbf{e}}_y \right] F^{(\ell n)}. \end{aligned} \quad (33)$$

Finally, we note $\mathbf{k} = (k \cos \phi, k \sin \phi)$ and $\mathbf{r} = (r \cos \theta, r \sin \theta)$ as well as the relation

$$\begin{aligned} \int \frac{d^2k}{(2\pi)^2} \exp(i\mathbf{k} \cdot \mathbf{r}) &= \int_0^{2\pi} \frac{d\phi}{2\pi} \int_0^\infty \frac{dk}{2\pi} \\ &\times k \exp[-ikr (\cos \theta \cos \phi + \sin \theta \sin \phi)]. \end{aligned} \quad (34)$$

Then the integration with respect to ϕ can be performed to obtain

$$\mathbf{v}(\mathbf{r}) = \hat{\mathbf{e}}_x \int_0^\infty dk \frac{J_1(kR) J_1(kr)}{2\pi \eta k R r [k^2 + \nu k \coth(kh)]} F^{(\ell n)}. \quad (35)$$

By identifying the velocity at the periphery of the domain to be \mathbf{U} and using Eq. (27), we obtain

$$\mathbf{U} = -\mathbf{F} \int_0^\infty dk \frac{J_1(kR)^2}{\pi\eta k R^2 [k^2 + \nu k \coth(kh)]}. \quad (36)$$

The friction coefficient is given by $\zeta = -\mathbf{F}/\mathbf{U}$. Following the Einstein relation $D = k_B T/\zeta$, we obtain the diffusion coefficient of a domain as

$$D_{\text{dom}} = k_B T \int_0^\infty dk \frac{J_1(kR)^2}{\pi\eta k R^2 [k^2 + \nu k \coth(kh)]}. \quad (37)$$

This is the generalization of the result obtained by De Koker to the case of finite solvent depth [39].

A. Limit of infinite thickness of the solvent layer

In this limit, the diffusion coefficient of the circular object was first calculated for the solid circular disk by Saffman and Delbrück [8, 9]. For a circular liquid domain which has the same viscosity as the outside of the domain, the diffusion coefficient was obtained by De Koker [39]. The similar expression was obtained for the domain shape relaxation times [46].

By taking the limit of $kh \gg 1$ in Eq. (10), the mobility tensor can be written as [22, 24]

$$G_{\alpha\beta}[\mathbf{k}] = \frac{1}{\eta(k^2 + \nu k)} \left(\delta_{\alpha\beta} - \frac{k_\alpha k_\beta}{k^2} \right). \quad (38)$$

If the above mobility tensor is used in Eq. (37), it reduces to that derived by De Koker [39]. In this case, the integration can be performed by using Mathematica with the use of Meijer G -functions [47]

$$D_{\text{dom}} = \frac{k_B T}{2\pi\eta(\nu R)^2} \left[-\frac{2}{(\nu R)^2} - 1 - \frac{1}{\pi^{3/2}} G_{24}^{32} \left[(\nu R)^2 \left| \begin{array}{c} 1/2, 3/2 \\ 0, 1, 3/2, -1 \end{array} \right. \right] \right]. \quad (39)$$

This expression is useful to take the limits with respect to νR .

In the case of $\nu R \ll 1$, the above expression reduces to

$$D_{\text{dom}} \approx \frac{k_B T}{4\pi\eta} \left[\ln \left(\frac{2}{\nu R} \right) - \gamma + \frac{1}{4} \right]. \quad (40)$$

The difference from the result by Saffman and Delbrück is the additional factor 1/4 in the r.h.s. of Eq. (40) [8, 9]. This means that the diffusion coefficient of a circular domain is

slightly larger than that of the disk, since the flow induced inside the domain reduces the friction between the membrane flow and the domain periphery compared to that between the membrane flow and the solid edge. In the opposite limit of $\nu R \gg 1$, the diffusion coefficient is obtained as

$$D_{\text{dom}} \approx \frac{4k_{\text{B}}T}{3\pi^2\eta_{\text{s}}R}, \quad (41)$$

which is inversely proportional to the domain radius, R . The obtained diffusion coefficient is again slightly larger than that of the disk in the same limit [10, 11]

$$D_{\text{disk}} \approx \frac{k_{\text{B}}T}{8\eta_{\text{s}}R}. \quad (42)$$

The fact that D_{dom} is inversely proportional to R is consistent with the result of 2D polymer chain in the membrane [28].

B. The limit of thin solvent layer

The diffusion in supported membranes in the $\nu h \ll 1$ limit was originally considered by Evans and Sackmann for the solid disk immersed in the membrane [14]. The diffusion coefficient of a circular viscous domain embedded in the membrane was recently studied by us [16]. In this case, Eq. (10) takes the following form

$$G_{\alpha\beta}[\mathbf{k}] = \frac{1}{\eta(k^2 + \kappa^2)} \left(\delta_{\alpha\beta} - \frac{k_{\alpha}k_{\beta}}{k^2} \right), \quad (43)$$

where $\kappa \equiv (\nu/h)^{1/2}$. The above mobility tensor was previously used by us [15–19].

We replace $\nu k \coth(kh) \simeq \kappa^2$ for $h \rightarrow 0$ in the integrand of Eq. (37). A rigorous condition of small h needs some care since $\kappa = (\nu/h)^{1/2}$ diverges in the limit of $h \rightarrow 0$ when ν is finite. In the previous section, we have discussed the condition in detail and shown that the results are valid under the condition given by $\nu h < 1$. With this replacement, we obtain

$$D_{\text{dom}} = \frac{k_{\text{B}}T}{\pi\eta(\kappa R)^2} \left[\frac{1}{2} - I_1(\kappa R)K_1(\kappa R) \right], \quad (44)$$

which coincides with our previous result [16]. However, it should be noted that the diffusion coefficient was obtained by taking into account the hydrodynamic force from the membrane alone in Ref. [16]. In order to compare the present result with our previous result, the direct friction between the solvent and the domain, $\pi\eta(\kappa R)^2$, should be added to the previous

result. This leads to add $k_B T / \pi \eta (\kappa R)^2$ to the diffusion coefficient. For comparison, we also write the result by Evans and Sackmann [14]

$$D_{\text{ES}} = \frac{k_B T}{\pi \eta (\kappa R)^2} \left[2 + \frac{4K_1(\kappa R)}{\kappa R K_0(\kappa R)} \right]^{-1}, \quad (45)$$

where the direct friction between the solvent and the domain is added. As pointed out before, Eq. (44) is slightly larger than Eq. (45) [16]. This is because the fluid flow in the domain reduces the friction between the domain and the host membrane at the edge.

In the limit of $\kappa R \ll 1$, the previous result is reproduced [16]

$$D_{\text{dom}} \approx \frac{k_B T}{4\pi \eta} \left[\ln \left(\frac{2}{\kappa R} \right) - \gamma + \frac{1}{4} \right]. \quad (46)$$

In the opposite limit of $\kappa R \gg 1$, the diffusion coefficient is obtained as

$$D_{\text{dom}} \approx \frac{k_B T}{2\pi \eta (\kappa R)^2}. \quad (47)$$

In this limit, D_{dom} decays as $1/R^2$ as pointed out before [16].

C. Finite thickness of solvent layer

In the case of finite h , the integration of Eq. (37) can be transformed into the summations as employed before

$$D_{\text{dom}} = \sum_{j=1}^{\infty} C_j \frac{k_B T}{\pi \eta (\kappa_j R)^2} \left[\frac{1}{2} - I_1(\kappa_j R) K_1(\kappa_j R) \right], \quad (48)$$

where C_j is the weight factor given by Eq. (17) and κ_j is determined by Eq. (16).

When $\nu h < 1$, C_j decreases rapidly as j increases as already shown in the previous section. In this case, Eq. (48) can be approximated by the lowest order expression,

$$D_{\text{dom}} \approx C_1 \frac{k_B T}{\pi \eta (\kappa_1 R)^2} \left[\frac{1}{2} - I_1(\kappa_1 R) K_1(\kappa_1 R) \right], \quad (49)$$

where κ_1 is the smallest positive value of κ_j . For $\kappa_1 R \ll 1$, Eq. (49) reduces to

$$D_{\text{dom}} \approx C_1 \frac{k_B T}{4\pi \eta} \left[\ln \left(\frac{2}{\kappa_1 R} \right) - \gamma + \frac{1}{4} \right], \quad (50)$$

whereas for $\kappa_1 R \gg 1$, it reduces to

$$D_{\text{dom}} \approx C_1 \frac{k_B T}{2\pi \eta (\kappa_1 R)^2}. \quad (51)$$

When $\nu h > 1$, Eq. (49) approximates the exact expression, Eq. (48), only when the expression multiplied to C_j rapidly decreases with increasing j as we have already stated in the previous section. Since the hydrodynamic screening lengths and the weights factors are common, the difference between the polymer and the circular liquid domain originates from the non-dimensional size dependence. However, the size dependence is very similar between the polymer and the circular domain, i.e., weak logarithmic dependence for relatively small sizes and the algebraic dependence at large sizes. As a consequence, essentially the same results as those shown in Fig. 4 are obtained for the two cases. The condition that the diffusion coefficient can be approximated by the expression with a single hydrodynamic screening length is essentially the same for the polymer and the circular liquid domain. When $\nu h > 1$, Eq. (51) is a good approximate expression of Eq. (48) but Eq. (50) is not.

Before closing the section, we compare in Fig. 6 the generalized solution of De Koker given by Eq. (37) with the results in the two limits; the original solution of De Koker obtained in the limit of $h \rightarrow \infty$ and the results of Eq. (44) obtained in the limit of $h \rightarrow 0$. The results of Eq. (37) with $\nu h = 0.1$ overlap with the results of Eq. (44). The diffusion coefficient of Eq. (44) is slightly larger than that of the solid disk, Eq. (45). By increasing νh the results shift toward the original solution of De Koker. In the asymptotic limit, the diffusion coefficient scales with $1/R^2$ in the generalized solution of De Koker, while the diffusion coefficient scales with $1/R$ in the the original solution of De Koker. In the opposite limit of $R \rightarrow 0$, all the results of Eq. (37) as well as the original solution of De Koker show the logarithmic dependence on R as represented by Eq. (40).

VI. CONCLUSIONS

The diffusion coefficient of an inclusion in a membrane is strongly influenced by the presence of solvents due to the stick boundary condition between the membrane and the solvent. The thickness of solvent layer is a key parameter controlling the diffusion of an inclusion in a membrane. In this work, the diffusion coefficient of a polymer confined in a membrane is obtained for arbitrary thickness of solvents. We also study the influence of finite thickness of solvent on the diffusion coefficient of a circular liquid domain with the same viscosity as that of the host membrane. Previously, the diffusion coefficient of a circular liquid domain was expressed by a single integral in the limit of infinite solvent thickness [39].

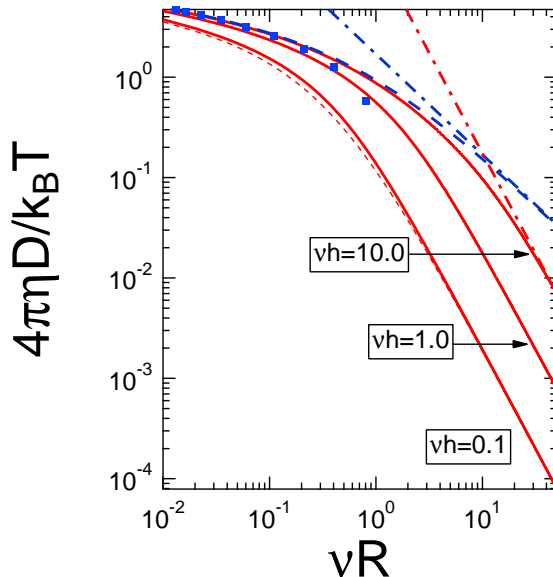


FIG. 6. (Color online) The diffusion coefficients of a liquid domain against size for various solvent thickness. The solid red lines represent the generalized solution of De Koker given by Eq. (37). $\nu h = 10$, $\nu h = 1$, and $\nu h = 0.1$ from right to left. The result in the limit of thin solvent layer, Eq. (44), overlaps with that of $\nu h = 0.1$. The red dashed-dotted line represents the asymptotic solution for $\nu h = 10$, Eq. (51). The red thin dashed line indicates the Evans-Sackman's expression, Eq. (45). The blue long dashed line represents the original solution of De Koker obtained by taking $h \rightarrow \infty$ limit in Eq. (37). The blue dots denote the results of Eq. (40) and the blue dashed-dotted line indicates the asymptotic results, Eq. (41).

In this work, the integral expression is generalized to the case of finite solvent depth. The various analytical expressions are obtained from the integral expression.

In general, the diffusion coefficient of inclusions decreases as the solvent thickness decreases. The solvent induces drag against the membrane flow, and as a result diffusion is suppressed. The drag increases as the distance between the membrane and the substrate decreases. More precisely, the influence of solvent on the membrane flow is characterized by the hydrodynamic screening lengths. Multiple hydrodynamic screening lengths can be obtained from the characteristic equation Eq. (16), when the solvent thickness is nonzero. The largest hydrodynamic screening length characterizes the length scale of momentum dissipation from the membrane to the solvent. The membrane flow dissipates the momentum to the solvent through the stick boundary condition. For finite solvent depth, the largest hy-

hydrodynamic screening length is approximately given by $\sqrt{h/\nu}$. The diffusion coefficients are expressed by the weighted sum of the functions of the non-dimensional size of the inclusion normalized by the hydrodynamic screening lengths. The weights are given by Eq. (17).

By examining both the weights and the non-dimensional size dependence, we find that the diffusion coefficient can be approximated by the expression given by the largest hydrodynamic screening length alone except when both ν^{-1} and the size of the inclusion are smaller than the solvent thickness. (The results are summarized in Table I.) When the solvent thickness is larger than ν^{-1} , $h > \nu^{-1}$, the weights decrease slowly with increasing j . Hence ν^{-1} can be viewed as the critical solvent depth below which there is a dominant mode given by the largest hydrodynamic screening length. If the size of the inclusion is smaller than the solvent thickness, $\kappa_1 R$ is close to $\kappa_2 R$ since we have $\kappa_2 R - \kappa_1 R \sim R/h$. Besides, if the diffusion coefficient depends weakly on $\kappa_j R$, the diffusion coefficient expressed by $\kappa_1 R$ alone cannot represent the exact summed result. In particular, the sum of logarithmic functions of screening lengths weighted by the similar factors cannot be represented by one of the terms. The situation is met when both ν^{-1} and the size of the inclusion are smaller than the solvent thickness.

The results summarized above are obtained for the finite solvent thickness. In the limit of $h \rightarrow \infty$, a new length scale appears as discussed by Diamant [25]. The diffusion coefficient is given by the new hydrodynamic screening length ν^{-1} .

For relatively small inclusions, the diffusion coefficients can be approximated by the logarithmic function of the size normalized by ES hydrodynamic screening length $\sqrt{h/\nu}$ when the solvent depth is small, i.e, $1/\nu > h$. In the opposite limit of $h \rightarrow \infty$, the diffusion coefficient is given by the logarithmic function of the size normalized by ν^{-1} . In the intermediate solvent depth, the diffusion coefficients are expressed by the sum of multiple terms and the diffusion coefficient cannot be represented by the logarithmic function of the largest hydrodynamic screening length. However, the diffusion coefficient may be approximated by a logarithmic function. This directs us to define an empirical interpolation of the effective hydrodynamic screening lengths by the inverse of $\kappa^* = \nu/(1 + \sqrt{\nu h})$ for any value of h when inclusions are small.

The size dependence of diffusion coefficients is influenced by the solvent depth. In the case of a supported membrane, the typical value of h is 20 Å and $\nu h \sim 10^{-2}$ can be estimated by introducing typical values of membranes; $\eta_s = 10^{-2}$ poise and η given by 1 poise multiplied

TABLE I. Summary of the size dependence of the diffusion coefficient when the solvent depth is finite.

amplitude separation ($h < 1/\nu$)	screening lengths separation ($h < R$)	solvent depth	domain size	size dependence
complete	— ^a	$h < 1/\kappa_1 < 1/\nu$	$R < 1/\kappa_1$	$\ln(\kappa_1 R)$
complete	— ^a	$h < 1/\kappa_1 < 1/\nu$	$1/\kappa_1 < R$	$1/(\kappa_1 R)^2$
incomplete	incomplete	$1/\nu < 1/\kappa_1 < h$	$R < h$	— ^b
incomplete	complete	$1/\nu < 1/\kappa_1 < h$	$h < R$	$1/(\kappa_1 R)^2$

^a The summation in the expression of the diffusion coefficient can be approximated by the dominant term as long as amplitude separation is complete no matter about the separation of screening lengths.

^b The summation in the expression of the diffusion coefficient cannot be approximated by a single dominant term. Even in the regime of $1/\kappa_1 < R < h$, $1/(\kappa_1 R)^2$ spatial dependence is not obtained.

by the membrane thickness $5 \times 10^{-3} \mu\text{m}$ [5]. This is the case when the ES hydrodynamic screening length Eq. (45) or its modification Eq. (44) are relevant. By using relatively large size of inclusion, $R > h = 20 \text{ \AA}$, the asymptotic $1/R^2$ dependence of diffusion coefficient can be observed.

In the case of vesicles of $10 \mu\text{m}$ size, $\nu h \simeq 1$ can be estimated by interpreting vesicle radius as solvent thickness [6]. Since the inclusion is normally smaller than the vesicle radius, we have $R/h < 1$. In this case, we can estimate as $\kappa R \sim \nu R/\sqrt{\nu h} < \sqrt{\nu h} \sim 1$. If the vesicle radius is regarded as a solvent thickness, it may be difficult to observe the asymptotic $1/R^2$ dependence of the diffusion coefficient. However, this estimation is not rigorous but is done just for the purpose of indicating the boundary effect caused by the finite radius of a vesicle. The real flow inside a vesicle should be different from that in the presence of the solid substrate. It should be also reminded that there is an additional difficulty to differentiate the translational diffusion of a domain from the rigid rotation of the vesicle [7].

For simplicity, we have considered the situation where the membrane is floated on a solvent layer. In general, both sides of a membrane are surrounded by solvents. We consider the case that the solvent layer on the membrane is covered by a substrate and is not a free standing film. We denote the 3D viscosity of solvent and the thickness in the upper domain as η_s^+ and h^+ , respectively, and those in the lower domain as η_s^- and h^- , respectively.

Equation (10) and Eq. (37) are valid if we replace $k + \nu \coth(kh)$ with $k + \nu^+ \coth(kh^+) + \nu^- \coth(kh^-)$, where $\nu^+ = \eta_s^+/\eta$ and $\nu^- = \eta_s^-/\eta$ [23]. Correspondingly, the characteristic equation becomes

$$\nu^+ \cot(\kappa_j h^+) + \nu^- \cot(\kappa_j h^-) = \kappa_j. \quad (52)$$

The influence of solvents on both sides of the membrane can be investigated by studying the roots of Eq. (52). By using $\cot x \approx 1/x$, we obtain

$$\kappa_1 = \sqrt{\frac{\nu^+}{h^+} + \frac{\nu^-}{h^-}}, \quad (53)$$

when $\kappa_1 h^+ < 1$ and $\kappa_1 h^- < 1$.

In the simple situation where the membrane is sandwiched by the same depth of solvent layers $h = h^+ = h^-$, both the characteristic equation, Eq. (16) and the weights given by Eq. (17) still hold by using the renewed definition of $\nu = \nu^+ + \nu^-$. The diffusion coefficients in this particular case can be obtained from those presented in this manuscript by substituting $\nu = \nu^+ + \nu^-$ [16].

If both h^+ and h^- are infinite, the screening length changes from κ_1^{-1} to $(\nu^+ + \nu^-)^{-1}$. Our study on the influence of the finite solvent thickness indicates that the diffusion coefficient can be approximately expressed in terms of κ_1 except when both the SD screening length and the size of the inclusion are smaller than both h^+ and h^- .

ACKNOWLEDGMENTS

We would like to thank Youhei Fujitani for fruitful discussions. This work was supported by KAKENHI (Grant-in-Aid for Scientific Research) on Priority Area ‘‘Soft Matter Physics’’ and Grant No. 21540420 from the Ministry of Education, Culture, Sports, Science and Technology of Japan.

APPENDIX: USEFUL RELATIONS

We have used the relations,

$$\int_0^{2\pi} \frac{d\varphi}{2\pi} \exp[-i(k_x \cos \varphi + k_y \sin \varphi) a] = J_0(ka) \quad (\text{A.1})$$

and

$$\begin{aligned} & \int_0^{2\pi} \frac{d\varphi}{2\pi} \exp[-i(k_x \cos \varphi + k_y \sin \varphi) a] \cos^2 \varphi \\ &= -\frac{1}{a^2} \frac{\partial^2}{\partial k_x^2} J_0(ka) = -\frac{k_x^2}{k^2} J_2(ka) + \frac{J_1(ka)}{ka}, \end{aligned} \quad (\text{A.2})$$

$$\begin{aligned} & \int_0^{2\pi} \frac{d\varphi}{2\pi} \exp[-i(k_x \cos \varphi + k_y \sin \varphi) a] \cos \varphi \sin \varphi \\ &= -\frac{1}{a^2} \frac{\partial^2}{\partial k_x \partial k_y} J_0(ka) = -\frac{k_x k_y}{k^2} J_2(ka). \end{aligned} \quad (\text{A.3})$$

-
- [1] P. Cicuta, S. L. Keller, and S. L. Veatch. *J. Phys. Chem. B.* **111** 3328 (2007)
 - [2] Y. Kaizuka and J.T. Groves, *Biophys. J.* **86**, 905 (2004)
 - [3] E. A. J.Reitz and J. J. Neefjes. *Nat. Cell Biol.* **3**, E145 (2001)
 - [4] Y. Gambin, R. Lopez-Esparza, M. Reffay, E. Sierecki, N. S. Gov, M. Genest, R. S. Hodges, and W. Urbach. *Proc. Natl. Acad. Sci. USA.* **103**, 2098 (2007)
 - [5] M. Tanaka, J. Hermann, I. Haase, M. Fischer, and S. G. Boxer, *Langmuir* **23**, 5638 (2007)
 - [6] M. Yanagisawa, M. Imai, T. Masui, S. Komura, and T. Ohta *Biophys. J.* **92** 115 (2007)
 - [7] S. Aliaskarisohi, P. Tierno, P. Dhar, Z. Khattari, M. Blaszczyński, and Th. M. Fischer, *J. Fluid Mech.* **654** , 417 (2010)
 - [8] P.G. Saffman and M. Delbrück, *Proc. Natl. Acad. Sci. USA* **72**, 3111 (1975)
 - [9] P.G. Saffman, *J. Fluid Mech.* **73**, 593 (1976)
 - [10] B.D. Hughes, B.A. Pailthorpe, and L.R. White, *J. Fluid Mech.* **110**, 349 (1981)
 - [11] E.P. Petrov and P. Schwille, *Biophys. J* **94**, L41 (2008)
 - [12] T. Izuyama, *Dynamics of Ordering Processes in Condensed Matter* Edited by S. Komura and H. Furukawa, p. 505 (Plenum, New York, 1988)
 - [13] Y.Y. Suzuki and T. Izuyama, *J. Phys. Soc. Japan* **58**, 1104 (1989)
 - [14] E. Evans and E. Sackmann, *J. Fluid Mech.* **194**, 553 (1988)
 - [15] K. Seki and S. Komura, *Phys. Rev. E* **47**, 2377 (1993)
 - [16] S. Ramachandran, S. Komura, M. Imai, and K. Seki, *Eur. Phys. J. E* **31**, 303 (2010)
 - [17] S. Komura and K. Seki, *J. Phys. II* **5**, 5 (1995)
 - [18] Y. Rserkovbyak and D.R. Nelson, *Proc. Natl. Acad. Sci. USA* **103**, 15002 (2006)

- [19] K. Seki, S. Komura, and M. Imai, *J. Phys.: Condens. Matter* **19**, 072101 (2007)
- [20] H. Stone and A. Ajdari, *J. Fluid Mech.* **369**, 151 (1998)
- [21] M. Haataja, *Phys. Rev. E* **80**, 020902(R) (2009)
- [22] K. Inaura and Y. Fujitani, *J. Phys. Soc. Jpn.* **77**, 114603 (2008)
- [23] S. Ramachandran, S. Komura, K. Seki, and M. Imai, *Soft Matter* **7**, 1524 (2011)
- [24] N. Oppenheimer and H. Diamant, *Biophys. J.* **96**, 3041 (2009)
- [25] H. Diamant, *J. Phys. Soc. Jpn.* **78**, 041002 (2009)
- [26] N. Oppenheimer and H. Diamant, *Phys. Rev. E* **82**, 041912 (2010)
- [27] S. Ramachandran, S. Komura, and G. Gompper, *Europhys. Lett.* **89**, 56001 (2010)
- [28] S. Ramachandran, S. Komura, K. Seki, and G. Gompper, *Eur. Phys. J. E* **34**, 11046-3 (2011)
- [29] A.J. Levine, T.B. Liverpool, and F.C. MacKintosh, *Phys. Rev. Lett.* **93**, 038102 (2004)
- [30] A.J. Levine, T.B. Liverpool, and F.C. MacKintosh, *Phys. Rev. E* **69**, 021503 (2004)
- [31] M. Muthukumar, *J. Chem. Phys.* **82**, 5696 (1985)
- [32] A. Naji, A.J. Levine, and P.A. Pincus, *Biophys. J.* **93**, L49 (2007) (2010)
- [33] Th. M. Fischer, *J. Fluid Mech.* **498**, 123 (2004)
- [34] K. Simons and E. Ikonen, *Nature* **387** 569 (1997)
- [35] D. A. Brown, and E. London, *Annu. Rev. Cell Dev. Biol.* **14** 111 (1998)
- [36] J.F. Klingler, H.M. McConnell, *J. Phys. Chem.* **97** 6096 (1993)
- [37] G. Orädd, P.W. Westerman, G. Lindblom, *Biophys. J.* **89** 315 (2005)
- [38] A.K. Kenworthy, B.J. Nichols, C.L. Remmert, G.M. Hendrix, M. Kumar, J. Zimmerberg, J. Lippincott-Schwartz, *J. Cell. Biol.* **165**, 735 (2004)
- [39] R. De Koker, *Domain structures and hydrodynamics in lipid monolayers. PhD dissertation*, Stanford University (1996).
- [40] Y. Fujitani, *J. Phys. Soc. Jpn.* **80**, 074609 (2011).
- [41] D.K. Lubensky, R.E. Goldstein, *Phys. Fluids* **8**, 843 (1996)
- [42] M. Doi, S.F. Edwards, *The Theory of Polymer Dynamics* (Clarendon press, Oxford, 1986)
- [43] F. John, *Comm. Pure and Appl. Math.* **1**, 45 (1950)
- [44] M. Abramowitz, I.A. Stegun, *Handbook of Mathematical Functions* (Dover, New York, 1972)
- [45] H.A. Stone, H.M. McConnell, *Proc. R. Soc. Lond. A* **448**, 97 (1995)
- [46] B.A. Camley, C. Esposito, T. Baumgart, and F.L.H. Brown, *Biophys. J.* **99** L44 (2010).
- [47] Wolfram Research Inc., *MATHEMATICA 8.0* (Wolfram Research, Champaign, 1988)